HHS Public Access

Author manuscript

Biochem J. Author manuscript; available in PMC 2016 March 01.

Published in final edited form as:

Biochem J. 2013 February 15; 450(1): 231–242. doi:10.1042/BJ20121612.

CATALYTIC DETOXIFICATION OF NERVE AGENT AND PESTICIDE ORGANOPHOSPHATES BY BUTYRYLCHOLINESTERASE ASSISTED WITH NON-PYRIDINIUM OXIMES

Zoran Radić[*], **Trevor Dale**[†], **Zrinka Kovarik**[‡], **Suzana Berend**[‡], **Edzna Garcia**[*], **Limin Zhang**[*], **Gabriel Amitai**[§], **Carol Green**[‖], **Božica Radić**[‡], **Brendan M. Duggan**[*], **Dariush Ajami**[†], **Julius Rebek Jr**[†], and **Palmer Taylor**[*]

[*]Skaggs School of Pharmacy and Pharmaceutical Sciences, University of California at San Diego, La Jolla, CA 92093

[†]Skaggs Institute for Chemical Biology and Department of Chemistry, The Scripps Research Institute, La Jolla, CA 92037

[‡]Institute for Medical Research and Occupational Health, HR-10001 Zagreb, Croatia

[§]Department of Pharmacology, Israel Institute for Biological Research, Ness Ziona 74100, Israel

[‖]SRI International, Menlo Park, CA 94025-3493

SYNOPSIS

We present here a comprehensive *in vitro*, *ex vivo* and *in vivo* study on hydrolytic detoxification of nerve agent and pesticide organophosphates (OPs) catalyzed by purified human butyrylcholinesterase (hBChE) in combination with novel non-pyridinium oxime reactivators. We identified 2-trimethylammonio-6-hydroxybenzaldehyde oxime (**TAB2OH**) as an efficient reactivator of OP-hBChE conjugates formed by the nerve agents, VX and cyclosarin, and the pesticide, paraoxon. It was also functional in reactivation of sarin and tabun inhibited hBChE. A three to five-fold enhancement of *in vitro* reactivation of VX, cyclosarin and paraoxon inhibited hBChE was observed, when compared to the commonly used *N*-methylpyridinium aldoxime reactivator, 2PAM. Kinetic analysis showed the enhancement resulted from improved molecular recognition of corresponding OP-hBChE conjugates by **TAB2OH**. The unique features of **TAB2OH** stem from an exocyclic quaternary nitrogen and a hydroxyl, both *ortho* to an oxime group on a benzene ring. pH dependences reveal participation of the hydroxyl (pK_a=7.6) forming an additional ionizing nucleophile to potentiate the oxime (pK_a=10) at physiological pH. The **TAB2OH** protective indices in therapy of sarin and paraoxon exposed mice were enhanced by

AUTHOR CONTRIBUTIONS

Zoran Radić, Julius Rebek Jr, Dariush Ajami, Trevor Dale and Palmer Taylor conceptually developed the project. Zoran Radić, Palmer Taylor, Julius Rebek Jr, Zrinka Kovarik, Gabriel Amitai Suzana Berend, Dariush Ajami, Carol Green and Brendan M. Duggan contributed to writing the paper. Julius Rebek Jr, Trevor Dale, Dariush Ajami and Gabriel Amitai designed and synthesized the oximes and fluorescent, non-volatile organophosphates. Zoran Radić, Palmer Taylor, Julius Rebek Jr, Zrinka Kovarik, Božica Radić and Carol Green contributed to the experimental design of the study. Zoran Radić, Edzna Garcia, Limin Zhang, Suzana Berend, Zrinka Kovarik and Brendan M. Duggan performed experiments and analysed the data.

30% – 60% when they were treated with a combination of **TAB2OH** and sub-stoichiometric hBChE. These results establish that oxime-assisted catalysis is feasible for OP bioscavenging.

Keywords

Oxime reactivation; organophosphate intoxication; butyrylcholinesterase reactivation; nonpyridinium oxime reactivators; catalytic organophosphate bioscavengers; edrophonium analogue

INTRODUCTION

Human exposure to organophosphates (OPs) is extensive and prevails as a global problem. The World Health Organization estimates that between 30,000 and 200,000 people die annually from acute OP poisoning [1], while more than 95% of the US population was found to be exposed to sublethal levels of OP based pesticides [2]. The exposure occurs largely through occupational exposure to OP-based pesticides, in attempted suicide with pesticides, by consuming improperly washed fruit or vegetables, but also from terrorist attacks with nerve gases, the most recent being one of 1995 in the Tokyo subway. More recently, several incidents of airplane passengers and crew being exposed to toxic jet-engine lubricant tri-o-cresylphosphate in “fume events” on board of commercial aircraft, were reported [3].

Exposure to OPs leads to covalent inhibition of cholinesterases (ChEs) in the peripheral and central nervous systems [4]. Common therapy of OP poisoning consists of symptomatic treatment with atropine and reactivation of OP inhibited acetylcholinesterase (AChE) by nucleophilic oxime antidotes. Frequently this therapy is limited by reinhibition of reactivated AChE by unreacted OPs that remain circulating in the blood following the exposure. To circumvent this problem the concept of bioscavengers, molecules that capture and degrade OPs in blood, has been introduced [5].

Oxime assisted recovery of catalytic activity has been studied in far greater detail for AChE, due to its physiological importance in neurotransmission than that of the closely related cholinesterase found in liver and plasma, butyrylcholinesterase (BChE). Consequently, most oxime reactivators developed to recover activity of OP-AChE conjugates are found less efficient in recovering OP-BChE activity [6, 7]. Interest in designing potent BChE reactivators has been stimulated recently with successful implementation of the “stoichiometric OP bioscavenger” approach based on administering purified human BChE to OP exposed animals [8–10].

Efficient protection of guinea pigs from multiple LD_{50} doses of nerve agents is found upon pretreatment with 20 – 30 mg/kg of purified human BChE. Similarly, antidotal administration of BChE to animals following OP exposure was demonstrated to provide effective protection. The effectiveness in protection is somewhat overshadowed by a common caveat of stoichiometric bioscavengers. Multi milligram quantities of large scavenger proteins are needed to remove stoichiometric equivalence of OP molecules of low molecular weight. The associated per dose cost and administration constraints for such

stoichiometric bioscavenger remain large. By enabling the BChE molecule to turn over multiple molecules of the OP, quantities of BChE needed for the effective protection could be significantly reduced and catalytic bioscavenger coverage could be provided for larger population of OP exposed individuals. We achieve this objective herein by simultaneous application of an efficient BChE reactivator, where the reactivating oxime assists BChE catalytic hydrolysis and turnover of the free organophosphate.

In this study we describe development of a prototypic catalytic OP bioscavenger based on combining purified human BChE with an efficient oxime reactivator with a distinctive structural scaffold. Starting with a small directed library of nonpyridinium, cationic, substituted benzenes, we identified an efficient reactivator of sarin, cyclosarin, VX, tabun and paraoxon derived OP-BChE conjugates and characterized kinetically its interaction with OP-BChE conjugates in detail.

EXPERIMENTAL

Enzyme

Highly purified recombinant monomeric hAChE was prepared as described earlier [7]. Purified human BChE isolated from human plasma was a gift from Drs. David Lenz and Douglas Cerasoli, USAMRICD. All enzyme concentrations given refer to concentration of catalytic sites i.e. monomers.

Organophosphates

Low toxicity, nonvolatile fluorescent methylphosphonates (Flu-MPs) [11] were used in *in vitro* experiments as analogues of nerve agents sarin, cyclosarin and VX. The Flu-MPs differ from actual nerve agent OPs only by structure of their respective leaving groups. Inhibition of hAChE by Flu-MPs results in OP-hAChE covalent conjugates identical to the ones formed upon inhibition with nerve agents. Paraoxon was purchased from Sigma-Aldrich (St. Louis MO, USA). Nerve agent OPs tabun, VX, sarin and soman used in *in vivo* experiments were purchased from NC Laboratory (Spiez, Switzerland).

Oximes

2PAM (2-Pyridinealdoxime methyl methanesulfonate or methiodide), and HI-6 (dichloride) were purchased from Sigma-Aldrich and US Biological (Swampscott, MA, USA).

Preparation of novel oximes

The edrophonium based antidotes **TAB2OH** and **TAB4OH** were synthesized from commercially available 3-dimethylaminophenol (Scheme S1). Protection of the phenol as the methoxymethyl (MOM) ether was completed in dichloromethane with chloromethyl methyl ether and DIEA. Product methoxymethyl ether was *ortho*-lithiated using *n*-butyllithium in ether at –40 °C and quenched with DMF to afford a mixture of 4-dimethylamino-2-methoxymethoxybenzaldehyde and 2-dimethylamino-6-methoxymethoxybenzaldehyde in an approximate 1:1.1 ratio, respectively. The regioisomers were separable by column chromatography over silica gel. Each isomer was separately converted to the oxime using hydroxylamine hydrochloride followed by removal of the

MOM group by heating in the presence of HCl in methanol. Finally, the 4-dimethylamino-2-hydroxybenzaldehyde oxime was quaternarized using an excess of iodomethane in hot THF to yield the desired trimethylanilinium derivative. The 2-dimethylamino-6-hydroxybenzaldehyde oxime was unreactive in the presence of iodomethane and required the more reactive electrophilic methyl source methyl triflate to quaternarize the aniline nitrogen. The triflate salt was anion exchanged for the chloride by exchange in an acetonitrile solution of tetrahexylammonium chloride which caused the product chloride to precipitate as a pure white solid.

Synthesis of the remaining seven novel oximes (Figure 1) is described in the Supplemental material, except for 4PyOHMOH which was synthesized as described earlier [12].

In vitro oxime reactivation assays

hAChE and hBChE activities were measured using a spectrophotometric assay [13] at 25 °C in 0.1 M sodium phosphate buffer, pH 7.4, containing 0.01% BSA and 1.0 mM substrate acetylthiocholine (ATCh). OP-hBChE and OP-hAChE conjugates were prepared and initial screening and detailed oxime reactivation experiments performed (at 37 °C in 0.1 M sodium phosphate buffer, pH 7.4, containing 0.01% BSA) as described earlier [7, 14]. The first order reactivation rate constant (k_{obs}) for each oxime + OP conjugate combination was calculated by nonlinear regression [15]. The dependence of reactivation rates on oxime concentrations and determination of maximal reactivation rate constant k_2, Michaelis-Menten type constant K_{ox} and the overall second order reactivation rate constant k_r were conducted as previously described [15].

pK_a determinations

Protonation of ionizable groups in the compounds was monitored by using UV/VIS spectrophotometry, by NMR spectrometry or by monitoring nucleophilic reactivity of the oxime group. A series of 20 mM phosphate-pyrophosphate buffers pH 5.0, 6.0, 7.0, 8.0, 8.5, 9.0, 9.5, 10, 10.5, and 11 (containing 0.1M NaCl) were prepared in either H_2O or D_2O. For D_2O buffers, pD values were determined by correcting the pH reading by + 0.4 pH units c.f. [16]. UV spectra of compounds between 220 nm and 320 nm wavelengths were recorded on a Cary 1E (Varian) UV/Vis spectrophotometer at the above pH values.

^1H NMR spectra recorded on Bruker Avance III 600 (Bruker, USA) spectrometer in 20 mM phosphate-pyrophosphate D_2O buffers pH 5.0, 6.0, 7.0, 8.0, 8.5, 9.0, 9.5 and 10 (containing 0.1M NaCl) were overlaid and aligned using benzene as an external standard placed in a separate capillary tube within the NMR sample probe. 2D ^1H-^1H COSY spectra were recorded on a Bruker Avance III 600 spectrometer.

Nucleophilic reactivity of oximes was determined in the above described buffers by measuring oxime induced rates of ATCh hydrolysis as detected by thiol reagent DTNB, by following time course of absorbance increase at 412 nm at room temperature (22 °C).

UV absorbance at discrete wavelengths, chemical shifts of discrete ^1H NMR peaks or rates of nucleophilic reactions were plotted as a function of pH yielding pK_a values by nonlinear regression of equation:

$$A = A^{max} / \left(1 + \left[H^+\right] / K_a\right) \quad \text{equation (1)}$$

or when the dependence on pH involved two ionization equilibria using equation:

$$A = {A_1}^{max} / \left(1 + \left[H^+\right] / K_{a1}\right) + {A_2}^{max} / \left(1 + \left[H^+\right] / K_{a2}\right) \quad \text{equation (2)}$$

Acute oxime toxicity and oxime treatment of OP exposed mice

Male CD-1 mice of 25–30 g body weight (purchased from Rudjer Bošković Institute, Zagreb, Croatia) fed on a standard diet, had free access to water and were kept in Macrolone cages at 21 °C, exchanging light and dark cycles every 12 h. Mice were randomly distributed into groups of four for each dose.

Acute intramuscular (i.m.) toxicity (LD_{50}) of **TAB2OH** was based upon 24 h mortality rates upon administration of four different doses of **TAB2OH**, one per each group of four mice, and calculated according to Thompson [17] and Weil [18].

The therapeutic efficacy of **TAB2OH** against OP poisoning was tested by administering mice (i.m.) with **TAB2OH** (10 or 25 mg/kg) together with atropine sulfate (10 mg/kg), one minute after subcutaneous (s.c.) OP exposure [19, 20]. Nerve agent stock solutions were prepared in isopropyl alcohol or in propylene glycol. Immediately before use, further dilutions were made in physiologic saline.

Alternatively, a combination of pretreatment and therapy was performed by intravenous (i.v.) application of hBChE (0.5 or 1.0 mg/kg) or combination of hBChE and **TAB2OH** (25 mg/kg) 15 or 30 min before s.c. OP exposure and then by i.m. administration of TAB2OH and atropine. The design of individual experiments is detailed in Table 4.

Antidotal efficacy of the oximes was expressed as a Protective Index (PI) with 95% confidence limits and maximal dose of organophosphate affording protection (MDP). The PI was the ratio of LD_{50} exerted by OP with antidote and OP given alone. The MDP was the highest multiple of the OP LD_{50}, which was fully counteracted by the antidotal treatment applied. The mice were treated in accord with the approval of the Ethical Committee of the Institute for Medical Research and Occupational Health in Zagreb, Croatia.

Oxime pharmacokinetics in mice

Female CD-1 mice 4–8 weeks old (19–27 g body weight) were purchased from Charles River (Hollister, CA). Mice were fed Purina Certified Rodent Chow #5002. Food and purified water was provided *ad libitum*. Mice were kept in hanging polycarbonate cages at 21–23°C, exchanging light and dark cycles every 12 h. General procedures for animal care and housing were in accordance with the National Research Council (NRC) Guide for the Care and Use of Laboratory Animals (1996) and the Animal Welfare Standards incorporated in 9 CFR Part 3, 1991.

In the experiments the mice were divided into groups of three. For pharmacokinetic studies, 30 mg/kg **TAB2OH** oxime was administered i.m. using 30mg/ml stock solution in a single dose in the absence of OP. Three animals were injected for every time point analyzed. Brain and plasma were collected at each time point. Blood (~300 μl) was collected from the retro-orbital sinus of mice under isoflurane anesthesia into tubes containing EDTA, processed to plasma within 30 minutes of collection, and then stored frozen at ≤−80°C (±10°C).

Brains were collected from each mouse at each time point (without perfusion of residual brain blood with saline). Brain weight was documented for each animal prior to storage on dry ice. Brains were stored at ≤−80°C (± 10°C) until analysis.

Concentration of the oxime in body compartments was determined by LC-MS using multiple reaction monitoring (MRM) electrospray ionization detection in positive ion mode. The peak transition 194.9 → 107.8 (m/z) at 19 eV collision energy and ~ 3.0 min retention time was monitored on the Micromass Quatro LC instrument (Micromass UK Limited, UK).

RESULTS

Structural design of the oxime library

A small directed library of cationic oxime reactivators was designed largely based on the base structure of the established reversible cholinesterase (ChE) inhibitor, edrophonium (Figure 1). Three structural elements were systematically varied in the eight compounds of the library including, position of the aldoxime group *ortho* or *para* to the quaternary substitution on the benzene ring, the presence or absence of a hydroxyl group vicinal to the aldoxime, and the size of the alkyl substitution on the exocyclic quaternary nitrogen (trimethyl, diethyl methyl or dimethyl ethyl). Of the two remaining oximes one was based on the structure of known reactivator 2PAM where a hydroxyl group was introduced into the *meta* position of the pyridinium ring vicinal to the aldoxime group (**2PAMOH**; Figure 1). In the other, two hydroxyl groups were introduced in *meta* positions, the oxime group in *para* and a methyl group in the *ortho* position (**4PyOHMOH**; Figure 1).

Reactivation screen of OP-hAChE and OP-hBChE conjugates by oximes of the directed library *in vitro*

Most oximes of the directed library were less effective than reference oximes 2PAM and HI6 in reactivation of OP-hAChE conjugates resulting from paraoxon, cyclosarin, VX or sarin inhibition (Figure 2A) as judged by screening procedures [14]. Only **TAB4OHmee** oxime was significantly better than 2PAM in reactivating an OP-hAChE conjugate. An order of magnitude enhancement in reactivation of cyclosarin inhibited hAChE by **TAB4OHmee** pointed to the importance of the unique combination of structural elements absent in the other evaluated oximes (Figure 1) including: bulky symmetrical quaternary nitrogen substitution, *para* substituted oxime group, and presence of a vicinal hydroxyl group. Nevertheless reactivation rates by **TAB4OHmee** were still less than HI-6, the best hAChE reactivator in this group of oximes, by an order of magnitude (Figure 2A).

Comparative analysis of reactivation for OP-hBChE conjugates of paraoxon, cyclosarin, VX or sarin, revealed efficacious reactivation by the oxime **TAB2OH**, faster than reactivation

by either of the two reference oximes 2PAM or HI-6, for all OPs except for sarin (Figure 2B). Thus, trimethylammonio benzene substituted with an aldoxime in the *ortho* position and hydroxyl group at an adjacent position provided a suitable structural template for efficient interaction with OP-hBChE conjugates. The omission of the adjacent hydroxyl (**TAB2**), the shift of the oxime to the *para* position (**TAB4OH** and **TAB4**) or shift of the exocyclic quaternary nitrogen into the ring to convert benzene into pyridinium (**2PAMOH**) all resulted in the loss of favorable reactivation potency observed for paraoxon, VX and cyclosarin hBChE conjugates (Figure 1, Figure 2B). Notably, the favorable influence of the shift of a delocalized positive charge in the pyridinium ring to an exocyclic, spherically-diffused charge distribution suggests that oxime/phenolate stabilization in OP-hBChE conjugates prefers a cation – π interaction with aromatic side chains, rather than π – π stacking of the two delocalized ring systems.

Reactivation kinetics of *TAB2OH* oxime *in vitro*

Comparative analysis of reactivation by a wide range of **TAB2OH** concentrations for OP-hBChE conjugates (0.1mM-10mM; Figure 3) and OP-hAChE conjugates (5 mM – 50 mM; Figure S1) confirmed the preferences observed in initial screening. Evaluation of individual reactivation constants k_2 and K_{ox} (Table 1) reveals that superior reactivation of OP-hBChE conjugates compared to 2PAM and faster reactivation of OP-hBChE compared to OP-hAChE conjugates; both largely reflect an improved binding interaction of **TAB2OH** to OP-hBChE conjugates (smaller K_{ox}). Both 2PAM and **TAB2OH** bind equally well to native hAChE and native hBChE as reflected in a K_is value of 0.2 – 0.3 mM (Table 1). Covalent OP conjugation differentially affects affinity for the two enzyme conjugates, lowering the affinity of **TAB2OH** for OP-hBChE only several-fold, but by two orders of magnitude for OP-hAChE. Association of 2PAM is about an order of magnitude weaker in either OP-hAChE or OP-hBChE conjugates. The overall difference in maximal reactivation rate constants for the two enzyme conjugates was smaller. Except for reactivation of hBChE conjugates of sarin and tabun,, maximal reactivation rates for **TAB2OH** were similar or larger than those determined for 2PAM.

In this analysis we assume that K_{ox} primarily describes initial reversible interaction of oxime reactivator with an OP-hAChE conjugate, whereas k_2 refers to the interaction of the reactivating oxime with the methyl phosphonate or diethyl phosphorate of the OP conjugated enzymes in forming the transition state of reactivation.

pK_a determinations

Structures of the lead hBChE reactivator **TAB2OH**, and several structurally related oximes (Figure 1) include two ionizable groups in the physiologically relevant pH range with the nucleophilic potential to affect the reactivation efficacy, the oxime group and the phenolic hydroxyl, that form the respective oximate and phenolate species. We determined pK_a values of ionizable groups for **TAB2OH**, structurally related oximes, **TAB2, TAB4OH, TAB4**, the structurally related reversible inhibitor, edrophonium, and reference oxime, 2PAM.

The bathochromic shift in the UV/VIS spectra, resulting from deprotonation of oxime and hydroxyl groups or from their protonation, enabled pK_a value determinations from an incremental increase in absorbance at discrete wavelengths (Figure S2; Table 2). For all compounds with single ionizable groups (**TAB2, TAB4,** 2PAM and edrophonium) the pH dependence of the absorbance change was consistent with a single ionization equilibrium at all peak wavelengths. For the ring substitutions containing the phenolic and aldoxime hydrogens, the pH dependence of the spectral change showed evidence for two ionization states, and allowed a simultaneous evaluation of pK_a values for both oxime and hydroxyl hydrogens (Figure S2; Table 2).

^{1}H NMR spectroscopy in D_2O was also used to monitor pH-dependent chemical shifts in reactivator resonance spectra, and confirmed the pK_a values of ionizable groups of the lead hBChE reactivator **TAB2OH** and the reference oxime, 2PAM (Figure S4; Table 2). The NMR pD range used (5.5 –10.5) allowed determination of only one pK_a value per compound. The chemical shift and appearance of five peaks in the **TAB2OH** spectrum were analyzed (Figure S3), two singlets (amido proton and nine equivalent trimethyl quaternary N protons), two doublets (aromatic benzene protons at ~ 7.2 ppm and ~7.42 ppm; at pH 5.0) and a triplet (aromatic benzene proton at ~ 7.52 ppm at pH 5.0). All five peaks shifted to lower ppm values with increasing pH and yielded pK_a values in the range of 7.63 – 7.74 (Figure S4, Figure S5, Table 2), thus reflecting deprotonation of the same group – the benzene hydroxyl. In the ^{1}H NMR spectrum of 2PAM in D_2O, the aldoxime CH and all aromatic proton signals shifted simultaneously, yielding a pK_a value of 8.11 [16]. The *N*-methyl peak at 2.8 ppm did not shift (Figure S6). Accordingly, the ionization state of the oxime group affects delocalization of the aromatic ring system of 2PAM, but not electron distribution around its *N*-methyl protons. The ionization state of **TAB2OH** phenolic hydroxyl influences the distribution of electrons and charge of the entire molecule, including the oxime group. The π– orbital interactions between delocalized ring electrons of reactivators and aromatic residues in the AChE gorge, and consequently binding orientations of these two structurally similar reactivators, endo- and exocyclic quaternary amines, thus appear to be different.

pH dependence of kinetics of catalysis

Nucleophilic reactivity and pK_a values for these compounds were additionally monitored by determining the rates of free oxime-induced catalysis (oximolysis) of ATCh, measured spectrophotometrically by the Ellman reagent DTNB (Figure 4; Table 2). Resulting profiles of the pH dependence for oximolysis exhibited two ionization equilibria for both hydroxyl oximes (**TAB2OH** and **TAB4OH**), but only a single one for **TAB2, TAB4** and 2PAM. No nucleophilic activity was detectable for edrophonium as judged by the absence of its influence on ATCh hydrolysis. The biphasic nucleophilic pH relationships for the two hydroxyl benzadehyde oximes (with pK_a values consistent with those determined for the oxime and hydroxyl groups using different approaches) indicate formation of a nucleophile at a pH close to the physiological range, in addition to the aldoxime group, and with its intrinsic reactivity significantly higher than that observed for the hydroxyl substitution alone on the benzene ring (Table 2). As a consequence, the nucleophilic strength of both hydroxyl

benzene aldoximes at physiological pH was enhanced in comparison to corresponding non-hydroxylated benzene aldoximes.

pK_a values determined for the same compounds using different methods were in good agreement. Moreover, pK_as of the oxime groupfor all four benzene aldoximes were not significantly different, irrespective of hydroxyl substitutions. Lastly, the hydroxyl group pK_as were identical for both phenolic oximes, in spite of differential substitution in the benzene ring. The hydroxyl group pK_a, on the other hand, appeared at least 0.6 pH units higher in the absence of the aldoxime group substitution, as evidenced by the edrophonium comparison. Finally, the pyridinium-based 2PAM oximate appeared to be stronger nucleophile at physiological pH than any of the benzene based oximates (Table 2), due to its lower (by two pH units) pK_a for the oxime to oximate dissociation.

Oxime assisted OP hydrolysis by hBChE *in vitro* and *ex vivo*

Hydrolysis of 5 μM solutions of racemic, fluorescent nerve agent OP analogues (Flu-MPs) by combinations of (500 nM hBChE + 100 μM oxime), as monitored by release of fluorescent OP leaving groups, reveals substantial breakdown of all four tested nerve agent analogues (cyclosarin, VX, sarin and soman) within the first few minutes of the reaction (Figure 5). The initial fast phases of hydrolysis by cyclosarin and VX likely correspond to complete degradation of more toxic, fast inhibiting and fast reactivating P_S OP enantiomers [21, 22] whereas the slow phase represents the sum of non-enzymic OP oximolysis and slow hBChE inhibition/reactivation by less reactive P_R enantiomers. For the soman analogue, the short initial fast phase corresponds to OP degradation before completion of aging of the soman-hBChE conjugate. OP hydrolysis assisted by **TAB2OH** was substantially faster than hydrolysis assisted by 2PAM, for cyclosarin and VX. The hydrolysis of the sarin analogue was slowest (except for the soman analogue). It was slightly better assisted by 2PAM, consistent with reactivation experiments (Figure 3), and largely monophasic. Non-enzymatic OP oximolysis, largely equivalent to slow reaction phases (Figure 5), was about two-fold faster for 2PAM compared to **TAB2OH** (data not shown), consistent with its stronger nucleophilic reactivity observed against ATCh at pH 7.4 (Figure 4, Table 2).

Thus, the combination of 500 nM hBChE and 100 μM **TAB2OH** was capable of catalyzing the complete degradation of 2.5 μM VX and cyclosarin analogues (half of 5 μM racemic OP) within 20 minutes, under physiological conditions (Figure 5; Table S2). Hydrolysis assisted by combination of 500 nM hBChE and 100 μM 2PAM was about four to five times slower (Table S2).

OP hydrolysis *ex vivo* monitored in human blood shows significant OP degradation and consequential recovery of total cholinesterase activity within 10 minutes following addition of 100 μM **TAB2OH**. The blood was initially supplemented with 300nM or 60 nM purified hBChE and subsequently exposed to 0.5 μM nerve agent Flu-MP OP analogue or paraoxon (Figure 6). The oxime, hBChE and OP concentrations in this experiment were selected to mimic respective concentrations likely to be found in the blood of an OP exposed person. Here 0.5 μM VX represents an equivalent of 935 μg VX in a 7.0 liter blood volume for a ~ 70 kg adult, or an equivalent of a 13 μg/kg i.v. dose which is 1.7-fold greater than the extrapolated LD_{50} value for humans [23] (assuming that all injected OP is transiently

retained in blood or vascular space). For hBChE, 60 – 300 nM range is an equivalent of actual 0.5 – 2.5 mg/kg i.v. dose, and this is about 10- to 50-fold lower than the dose recommended for administration of hBChE as a stoichiometric OP bioscavenger [24] in the treatment of an OP exposure. Within the initial ten minutes of **TAB2OH** assisted catalysis, the VX analogue concentration declined most rapidly (50 –70% recovered activity), followed by cyclosarin analogue and paraoxon (~ 30% recovered activity) and sarin analogue (~ 15% recovered activity).

Acute TAB2OH toxicity and treatment of OP exposed mice

We determined the acute i.m. toxicity for mice of the lead hBChE reactivator **TAB2OH** to be 100 mg/kg, comparable to that of 2PAM (LD_{50}=106 mg/kg; [16]), but more toxic than the common oxime reactivator HI-6 (LD_{50}=450 mg/kg) or our lead centrally active *N*-substituted hydroxyimino acetamido alkyl amine, RS194B (LD_{50}=500 mg/kg) [16].

OP exposed mice were treated i.m. with **TAB2OH** (a dose equal to 25% of its LD_{50} where no signs of intoxication were observed) in conjunction with atropine one minute after s.c. OP exposure. The mice were 5.0 times less sensitive to the dose of VX, 10 times less sensitive to paraoxon, 2.9 times less sensitive to sarin and 1.6 times less sensitive to tabun (Table 3). The corresponding indices for 2PAM were slightly better, with respective protective indices for VX, paraoxon, sarin and tabun of 9.3, 47, 6.7 and 1.3 [16]. This therapeutic efficacy appears surprisingly good and better by (on average) one order of magnitude than would be expected solely from comparison of *in vitro* OP-hAChE reactivation kinetics for 2-PAM and **TAB2OH** (Figure S1, Table 1). The respective second order reactivation rate constants of 2PAM were 23-fold, 3.7-fold, 97-fold and 9.7-fold larger than TAB2OH reactivation rate constants for the respective OP-AChE conjugates:VX, paraoxon, sarin and tabun (Table 1), while ratios of respective protective indexes between 2PAM and **TAB2OH** therapies were 1.9, 4.7, 2.3 and 0.81 (Table 3). Thus a question could be raised on the vital importance of reactivation of OP-hBChE conjugates in peripheral tissues accessible to the charged reactivators **TAB2OH** and 2PAM, for survival in OP intoxication.

Pretreatment of mice with combination of 25 mg/kg **TAB2OH** and 1 mg/kg purified hBChE 15 min prior to OP exposure followed by therapeutic administration of another 25 mg/kg of **TAB2OH** in conjunction with atropine (10 mg/kg im) 1 min post OP did not provide notable protection in VX and tabun exposed mice. However, significantly (judged by 95% confidence limits; Tables 3 and 4) higher protective indices were observed for paraoxon (59% increase) and sarin (38% increase) when compared to the oxime therapy alone (in conjunction with atropine). The *in vitro* determined K_{ox} values for **TAB2OH** and OP-hAChE conjugates are in the 8–36 millimolar range, about one thousand times higher than the measured 10 μM **TAB2OH** concentrations in plasma. Accordingly, the observed Protective Index increase cannot be ascribed to the protective effect of the native hAChE from OP inhibition by **TAB2OH**. Rather, we ascribe the increase to *catalytic* degradation of OP in plasma mediated by the combination of sub-stoichiometric amounts of hBChE and **TAB2OH**. To verify this conclusion we varied the timing and administration regime of hBChE and **TAB2OH** to mice during and after OP exposure (Table 4). As expected,

pretreatment of mice by sub-stoichiometric doses of hBChE alone did not influence protective indices, except when it was administered together with atropine. On the other hand, whenever sub-stoichiometric hBChE was administered together with **TAB2OH** (and with atropine), either as a pretreatment before paraoxon or as a therapy post paraoxon exposure, the resulting protective indices were higher (significantly considering 95% confidence limits) by 30% to 60% than in the treatment without hBChE (Table 4) but with atropine.

TAB2OH pharmacokinetics in mice

The highest concentration of **TAB2OH** determined in plasma upon i.m. administration of a single dose of 30 mg/kg was 2.2 μg/ml (or ~ 10μM), observed at the initial, 15 min collection point (Figure S7; Table S1). The decline from the plasma is rapid and appears multiphasic, precluding an initial estimate of the volume of distribution after i.m. dosing. As expected for a quaternary cation, blood-brain barrier (BBB) penetration appeared minimal. Maximal brain concentration determined at the 15 min collection point was 0.13 μg/ml (equivalent to ~0.56 μM) or about 18-fold lower than in plasma. Retention of the low concentrations of **TAB2OH** that appear to have penetrated into the brain, however, was prolonged. While kinetics of elimination by mice is typically more rapid than in humans, the high plasma clearance rate of **TAB2OH** may necessitate either multiple dosing or a single dose of a pharmaceutical formulation of the oxime affording sustained release from the administration site.

DISCUSSION

Our data presented here describe the initial design, synthesis and detailed *in vitro* and *in vivo* characterization of a novel, effective reactivator of phosphylated hBChE: cationic quaternary oxime **TAB2OH**. Identified from a directed library of cationic oxime reactivators based on cholinesterase reversible inhibitor edrophonium, it proved four to five-fold more effective than the reference oxime 2PAM for *in vitro* reactivation of OP-hBChE conjugates of cyclosarin, VX and paraoxon. Dissection of reactivation rate constants revealed improved molecular recognition (reduced K_{ox}) to contribute most to the superior reactivation when compared either to 2PAM for reactivation of OP-hBChE conjugates or to **TAB2OH** reactivation of OP-hAChE conjugates.

Determinations of oxime group pK_a values for the two reactivators, however, reveal a much less dissociated oxime nucleophile of the **TAB2OH** reactivator (with average pK_a = 10) compared to 2PAM (with average pK_a = 8.1). Measurements of oxime nucleophilic reactivities by hydrolysis of both ATCh and Flu-MPs (Figure 4, Table 2, Table S2) in the absence of enzyme at pH 7.4 show only two to three-fold difference between the two oximes due to biphasic dependence on pH for **TAB2OH** reactivation. The lower pK_a of 7.21 evaluated from this biphasic dependence coincides with the lower of the two pK_a values observed from pH dependence of UV spectra of **TAB2OH** and its homologous hydroxyl oxime **TAB4OH**. This was not observed in monophasic pH dependences of their non-hydroxyl analogues **TAB2** and **TAB4** (Table 2, Figure 4) that reveal only a single pK_a value ~ 10 corresponding to the oxime group. The observed enhanced nucleophilic reactivity of

TAB2OH (and **TAB4OH**) at pH 7.4 thus appears as a consequence of deprotonation of the *ortho* substituted phenolic hydroxyl. Direct participation of nucleophilic reactivity of this hydroxyl *per se* in those reactions is, however, unlikely since the hydroxyl of structurally related edrophonium remains completely unreactive, even at pH 10 in it's nearly completely deprotonated form. Thus, a new non-aldoxime nucleophilic species or an activated aldoxime moiety due to intra-molecular interaction with the adjacent hydroxyl moiety, formed upon deprotonation of the hydroxyl *ortho* to the aldoxime, contributes to the unusual reactivity of **TAB2OH** and **TAB4OH** at physiological pH values.

One possible mechanism that could bridge between these two different pKa values and nucleophilicity of phenolate vs. oxime group could be the formation of an intermediate to a stabilized bicyclic ring comprised of two adjacent carbons of the benzene ring, the phenolate O^- and two atoms of the aldoxime, C=N-O-H. Such a transition state or meta-stable intermediate ring cyclization to form an isoxazole could form at pH=7.4. Alternatively the phenolate O^- in the active site might react with a terminal H from the CH=NOH group, leading to partial deprotonation of CH=NO-H and converting it into an oximate anion $CH=NO^-$ at physiological pH, the active nucleophile in reactivation of OP-ChE conjugates by aldoximes. Additional studies will be needed to identify the precise structural species and mechanistic nature of this functionally beneficial nucleophilic reaction. Enhanced nucleophilicity of *ortho* hydroxyl substituted benzene aldoximes, but with monophasic pH dependence and only limited *in vitro* reactivation potency has been observed elsewhere [25]. Additionally, hydroxyl groups positioned *ortho* to oxime reactivators enhance decomposition of phosphonyl-oximes, probably through intramolecular formation of an isoxazole ring [26, 27] and minimize eventual reinhibition of enzymes observed for some phosphonyl-oxime adducts [28].

A reasonable *in vitro* potency of **TAB2OH** for reactivation of OP-hBChE conjugates raises new considerations for establishing a catalytic OP bioscavenger based on **TAB2OH** assisted OP hydrolysis by hBChE. Our initial experiments demonstrate that both *in vitro* in physiologically conditioned buffers and *ex vivo* in the whole human blood, low micromolar and submicromolar OP concentrations (that could be expected to accumulate in blood of OP exposed individuals) are degraded significantly within 5 to 20 minutes of administration of 100μM **TAB2OH** and sub-stoichiometric (60–300 nM) hBChE. These results and moderate acute toxicity of **TAB2OH** (LD_{50} of 100 mg/kg i.m.) in mice allowed us to test this catalytic OP bioscavenger *in vivo* in nerve agent and OP pesticide exposed mice. Under varying administration regimens of **TAB2OH** and hBChE to the OP exposed mice, we observed 30% – 60% enhanced oxime protective indices whenever the BChE+ **TAB2OH** combination was administered to paraoxon exposed mice, either before paraoxon exposure (pretreatment) or after paraoxon exposure (therapy). No protection was observed for mice administered with sub-stoichiometric amounts of hBChE alone (without atropine), either in pretreatment or when administered therapeutically post OP. We assume that enhanced protective indices reflect catalytic turnover of paraoxon by (hBChE+ **TAB2OH**) combination acting as a catalytic bioscavenger.

The moderate extent of protective index enhancement for paraoxon, and the absence of the enhancement in the treatment of VX exposed mice likely reflect low tissue accumulation

and rapid clearance of **TAB2OH** from plasma. A maximal determined plasma concentration of 10 μM **TAB2OH** 15 min following a single 30 mg/kg i.m. administration (Figure S5) is likely insufficient to provide optimal assistance to hBChE in the OP turnover. To enhance efficacy in catalytic OP bioscavenging, a compound with lower toxicity and lower clearance than the **TAB2OH** lead would be beneficial. Nevertheless, our data with this lead show the "proof of principle" for effective catalytic OP bioscavenging based on combined administration of substoichiometric amounts of purified hBChE and an oxime reactivator. Such an approach would allow for significant cost reduction and more practical implementation of antidotal administration in treatment of OP exposure in high risk settings.

Supplementary Material

Refer to Web version on PubMed Central for supplementary material.

Acknowledgments

We thank Mr. Vedran Micek and Ms. Jasna Mileković for assistance with *in vivo* experiments and Ms. Valeria Gerardi for recording TAB2OH UV/VIS spectra.

FUNDING

This research was supported by the Counter ACT Program, National Institutes of Health Office of the Director (NIH OD), and the National Institute of Neurological Disorders and Stroke (NINDS), [Grant Numbers U01 NS058046 and R21NS072086].

REFERENCES

1. Eddleston M. Patterns and problems of deliberate self-poisoning in the developing world. Q. J. Med. 2000; 93:715–731.
2. Barr DB, Allen R, Olsson AO, Bravo R, Caltabiano LM, Montesano A, Nguyen J, Udunka S, Walden D, Walker RD, Weerasekera G, Whitehead RD Jr, Schober SE, Needham LL. Concentrations of selective metabolites of organophosphorus pesticides in the United States population. Environ. Res. 2005; 99:314–326. [PubMed: 16307973]
3. Liyasova M, Li B, Schopfer LM, Nachon F, Masson P, Furlong CE, Lockridge O. Exposure to tri-o-cresyl phosphate detected in jet airplane passengers. Toxicol. Appl. Pharmacol. 2011; 256:337–347. [PubMed: 21723309]
4. Taylor, P. Goodman & Gilman's The Pharmacological Basis of Therapeutics. 13th. Brunton, LL.; Chabner, B.; Knollman, B., editors. New York: McGraw-Hill; 2011. p. 239-254.
5. Ashani Y, Shapira S, Levy D, Wolfe AD, Raveh L. Butyrylcholinesterase and acetylcholinesterase prophylaxis against soman poisoning in mice. Biochem. Pharmacol. 1991; 41:37–41. [PubMed: 1986743]
6. Wiesner J, Kříž Z, Kuča K, Jun D, Koča J. Why acetylcholinesterase reactivators do not work in butyrylcholinesterase. J. Enzyme Inhib. Med. Chem. 2009; 25:318–322. [PubMed: 19874115]
7. Sit RK, Radić Z, Gerardi V, Zhang L, Garcia E, Katalinić M, Amitai G, Kovarik Z, Fokin VV, Sharpless KB, Taylor P. New structural scaffolds for centrally acting oxime reactivators of phosphylated cholinesterases. J. Biol. Chem. 2011; 286:19422–19430. [PubMed: 21464125]
8. Cerasoli DM, Griffiths EM, Doctor BP, Saxena A, Fedorko JM, Greig NH, Yu QS, Huang Y, Wilgus H, Karatzas CN, Koplovitz I, Lenz DE. *In vitro* and *in vivo* characterization of recombinant human butyrylcholinesterase (Protexia) as a potential nerve agent bioscavenger. Chem. Biol. Interact. 2005; 157–158:363–365.
9. Lenz DE, Yeung D, Smith JR, Sweeney RE, Lumley LA, Cerasoli DM. Stoichiometric and catalytic scavengers as protection against nerve agent toxicity: a mini review. Toxicology. 2007; 233:31–39. [PubMed: 17188793]

10. Mumford H, E Price M, Lenz DE, Cerasoli DM. Post-exposure therapy with human butyrylcholinesterase following percutaneous VX challenge in guinea pigs. Clin. Toxicol. (Phila). 2011; 49:287–297. [PubMed: 21563904]
11. Amitai G, Adani R, Yacov G, Yishay S, Teitlboim S, Tveria L, Limanovich O, Kushnir M, Meshulam H. Asymmetric fluorogenic organophosphates for the development of active organophosphate hydrolases with reversed stereoselectivity. Toxicology. 2007; 233:187–198. [PubMed: 17129656]
12. Heyl D. Vitamin B6. V.Conversion of pyridoxine to the lactone of 4-pyridoxic acid. J. Am. Chem. Soc. 1948; 70:3434–3436. [PubMed: 18891882]
13. Ellman GL, Courtney KD, Andres V Jr, Featherstone RM. A new and rapid colorimetric determination of acetylcholinesterase activity. Biochem. Pharmacol. 1961; 7:88–95. [PubMed: 13726518]
14. Cochran R, Kalisiak J, Kucukkilinc T, Radić Z, Garcia E, Zhang L, Ho KY, Amitai G, Kovarik Z, Fokin VV, Sharpless KB, Taylor P. Oxime-assisted acetylcholinesterase catalytic scavengers of organophosphates that resist aging. J. Biol. Chem. 2011; 286:29718–29724. [PubMed: 21730071]
15. Kovarik Z, Radić Z, Berman HA, Simeon-Rudolf V, Reiner E, Taylor P. Mutant cholinesterases possessing enhanced capacity for reactivation of their phosphonylated conjugates. Biochemistry. 2004; 43:3222–3229. [PubMed: 15023072]
16. Radić Z, Sit RK, Kovarik Z, Berend S, Garcia E, Zhang L, Amitai G, Green C, Radić B, Fokin VV, Sharpless KB, Taylor P. Refinement of structural leads for centrally acting oxime reactivators of phosphylated cholinesterases. J. Biol. Chem. 2012; 287:11798–11809. [PubMed: 22343626]
17. Thompson WR. Use of moving averages and interpolation to estimate median-effective dose; fundamental formulas, estimation of error, and relation to other methods. Bacteriol. Rev. 1947; 2:115–145.
18. Weil A. Criteria for Linear Equivalence. Proc. Natl. Acad. Sci. USA. 1952; 38:258–260. [PubMed: 16589088]
19. Čalić M, Vrdoljak AL, Radić B, Jelić D, Jun D, Kuča K, Kovarik Z. In vitro and in vivo evaluation of pyridinium oximes: mode of interaction with acetylcholinesterase, effect on tabun- and soman-poisoned mice and their cytotoxicity. Toxicology. 2006; 219:85–96. [PubMed: 16332406]
20. Berend S, Katalinić M, Vrdoljak AL, Kovarik Z, Kuča K, Radić B. In vivo experimental approach to treatment against tabun poisoning. J. Enzyme Inhib. Med. Chem. 2010; 25:531–536. [PubMed: 20235800]
21. Hosea NA, Radić Z, Tsigelny I, Berman HA, Quinn DM, Taylor P. Aspartate 74 as a primary determinant in acetylcholinesterase governing specificity to cationic organophosphonates. Biochemistry. 1996; 35:10995–11004. [PubMed: 8718893]
22. Wong L, Radić Z, Brüggemann RJ, Hosea N, Berman HA, Taylor P. Mechanism of oxime reactivation of acetylcholinesterase analyzed by chirality and mutagenesis. Biochemistry. 2000; 39:5750–5757. [PubMed: 10801325]
23. Munro NB, Ambrose KR, Watson AP. Toxicity of the organophosphate chemical warfare agents GA, GB and VX: Implication for public protection. Environ. Health. Perspect. 1994; 102:18–38. [PubMed: 9719666]
24. Masson P, Lockridge O. Butyrylcholinesterase for protection from organophosphorus poisons; catalytic complexities and hysteretic behavior. Arch. Biochem. Biophys. 2010; 494:107–144. [PubMed: 20004171]
25. Saint-Andre G, Kliachyna M, Kodepelly S, Louise-Leriche L, Gillon E, Renard P-Y, Nachon F, Baati R, Wagner A. Design, synthesis and evaluation of new a-nucleophiles for the hydrolysis of organophosphorus nerve agents: application to the reactivation of phosphorylated acetylcholinesterase. Tetrahedron. 2011; 67:6352–6361.
26. Dale TJ, Rebek J Jr. Hydroxy oximes as organophosphorus nerve agent sensors. Angew. Chem. 2009; 121:7990–7992.
27. Dale TJ, Rebek J Jr. Hydroxy oximes as organophosphorus nerve agent sensors. Angew. Chem. Int. Ed. 2009; 48:7850–7852.

28. Luo C, Saxena A, Ashani Y, Leader H, Radić Z, Taylor P, Doctor BP. Role of edrophonium in prevention of the re-inhibition of acetylcholinesterase by phosphorylated oxime. Chem. Biol. Interact. 1999; 119–120:129–135.

The abbreviations used

BChE	butyrylcholinesterase
hBChE	human BChE
AChE	acetylcholinesterase
hAChE	human AChE
ATCh	acetylthiocholine
BSA	bovine serum albumin
OP	organophosphate
2PAM	2-pyridinealdoxime methiodide
MDP	maximal dose of poison
MOM	methoxymethyl
PI	protective index

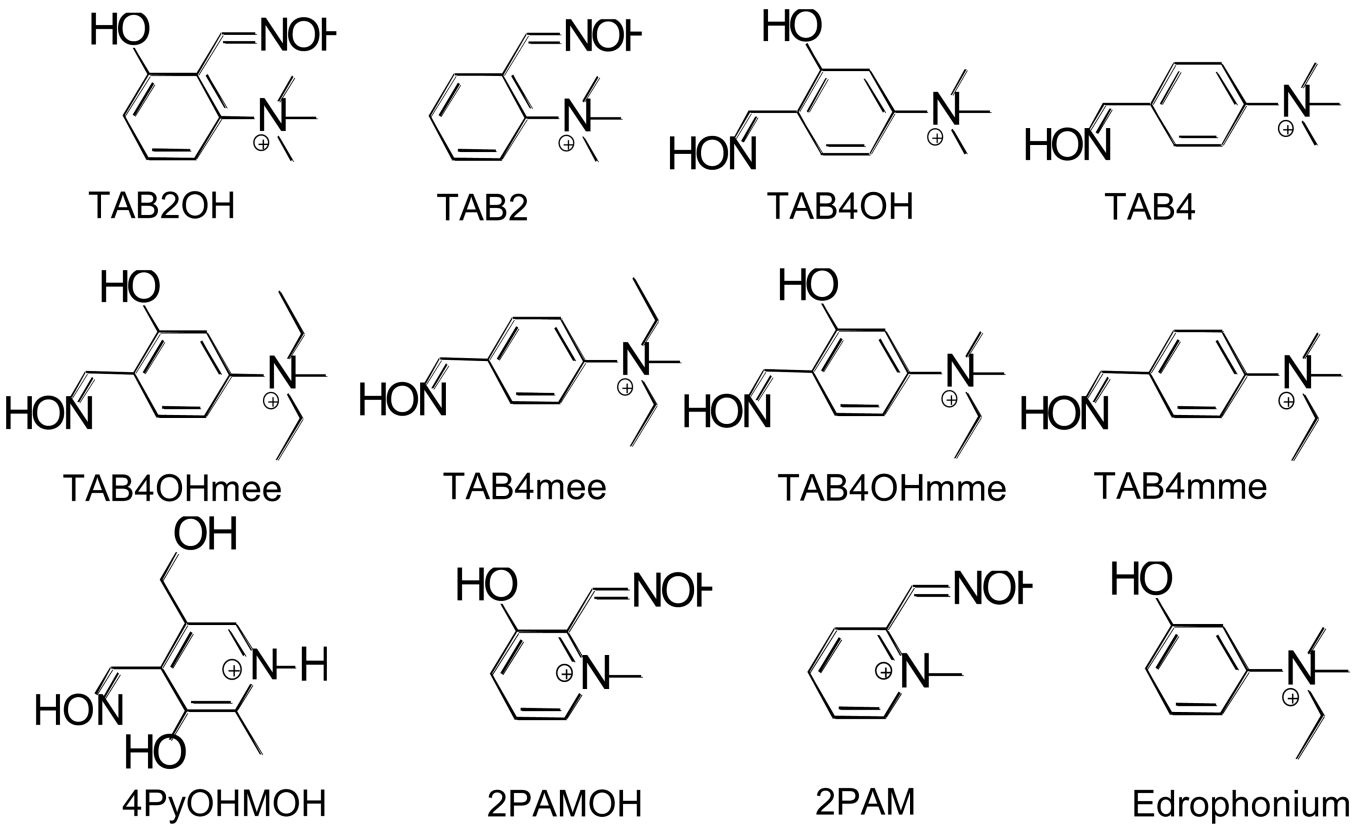

Figure 1.

Structures of novel oximes used in this study compared to structures of reference oxime 2PAM and reversible inhibitor edrophonium. Anions for all oximes and edrophonium were chloride except for 2PAM where anion was methanesulfonate.

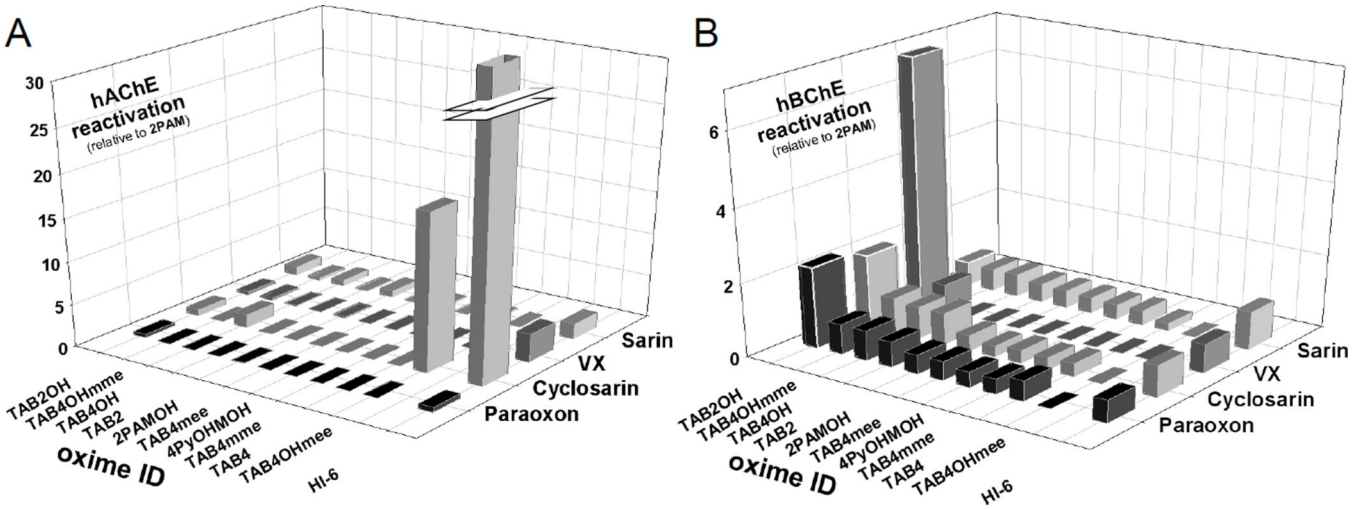

Figure 2.

Reactivation of paraoxon, cyclosarin, VX and sarin inhibited A) hAChE and B) hBChE by directed library of 10 novel oxime reactivators shown in Figure 1. Reactivation efficiencies of 0.67 mM oximes (measured in duplicate at 37 °C in 0.10M phosphate buffer pH 7.4) were determined using either ”take 5” (paraoxon, cyclosarin, VX inhibited hAChE and VX inhibited hBChE) or “quick-screen” (paraoxon, cyclosarin, sarin inhibited hBChE and sarin inhibited hAChE) assay procedures and are expressed relative to 2PAM reactivation efficiency. Cyclosarin, VX and sarin inhibited enzymes were formed by reaction with Flu-MPs yielding a conjugate identical to nerve agent inhibited enzymes (cf. Experimental section). The bar representing reactivation of cyclosarin inhibited hAChE conjugate by HI-6 (panel A) was truncated (the full height was 170) to allow for visualization of less efficient reactivation by other oximes.

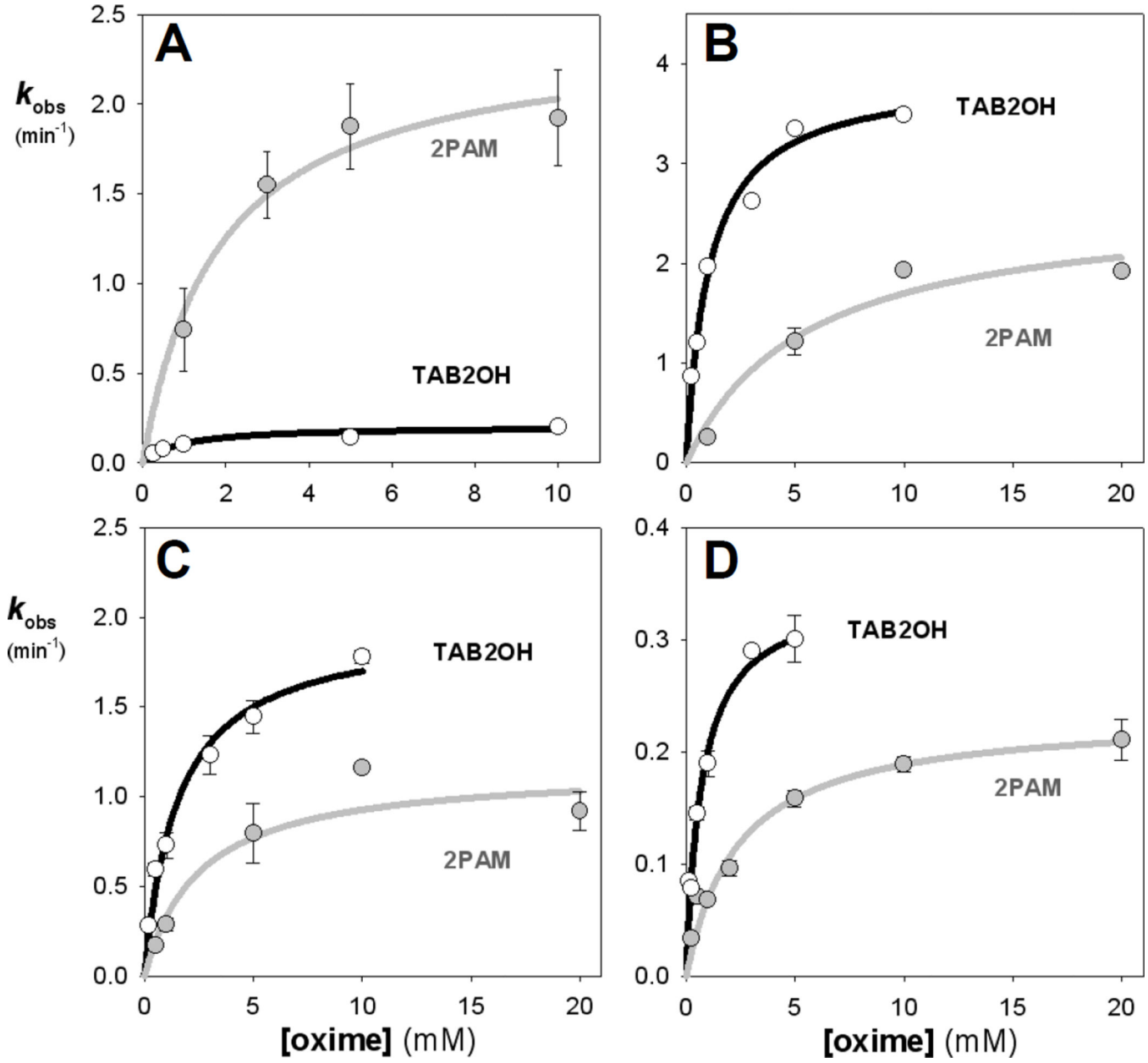

Figure 3.

Concentration dependence of oxime reactivation of **A)** sarin, **B)** cyclosarin, **C)** VX and **D)** paraoxon inhibited (conjugated) hBChE. Dependence for the lead oxime **TAB2OH** compared to reference cationic oxime 2PAM (measured in triplicate experiments at 37 °C in 0.10M phosphate buffer pH 7.4). Reactivation constants derived for each concentration dependence are given in Table 1. OP conjugates of sarin, cyclosarin and VX were formed by reaction with Flu-MPs and were identical to nerve agent inhibited enzymes (cf. Experimental section).

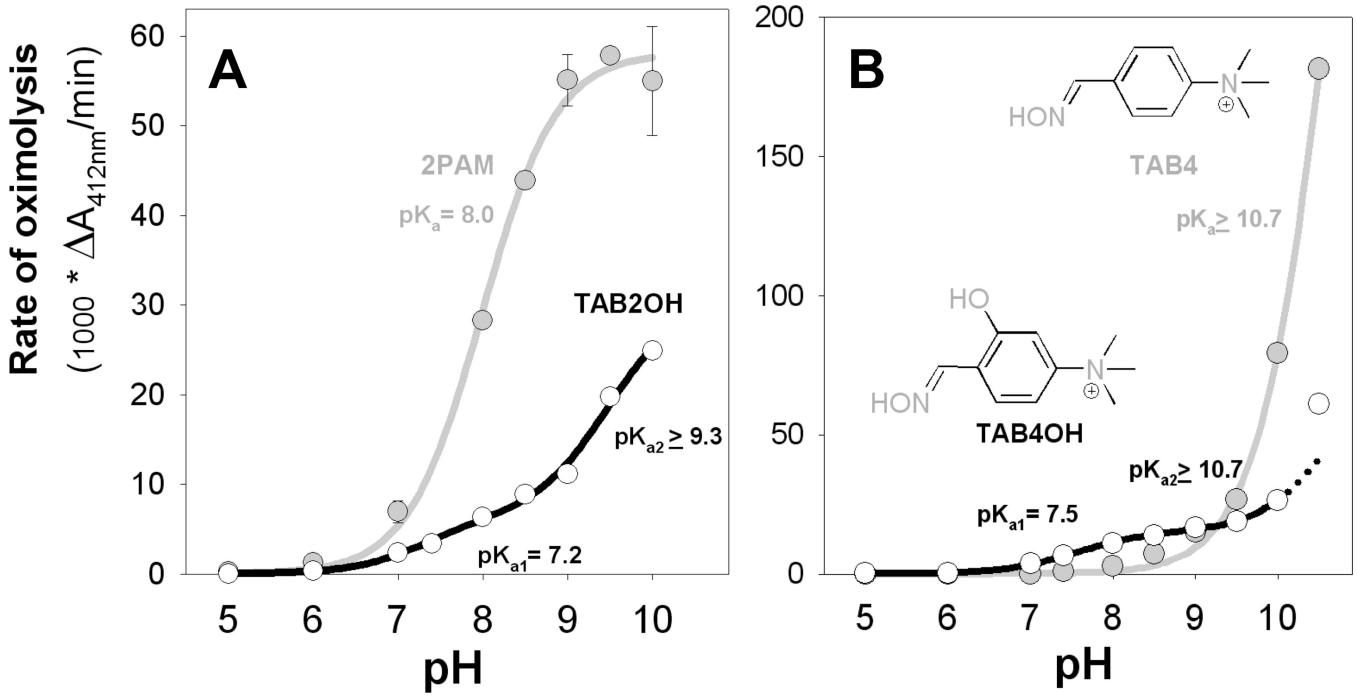

Figure 4.

pH dependence of rates of ATCh hydrolysis by oximes – oximolysis. Rates of 1 mM ATCh hydrolysis by **A)** 100 μM oximes TAB2OH, yielding biphasic pH dependence and reference oxime, 2PAM, yielding a monophasic dependence, and by **B)** 100 μM oximes TAB4OH and TAB4, yielding respective biphasic and monophasic pH dependences. Kinetics were measured spectrophotometrically in duplicates or triplicates at 22 °C in 20mM phosphate-pyrophosphate buffers (containing 100 mM NaCl) using Ellman reagent DTNB. Error of determination was smaller than the size of the symbol, except where indicated by error bars. Resulting pKa values calculated by nonlinear fit [16] are given in the figure and recorded in Table 2 together with associated errors. pK_{a2} values higher than 9 were presented as “larger or equal” since rates of oximolysis were measured up to pH 10 or 10.5, only.

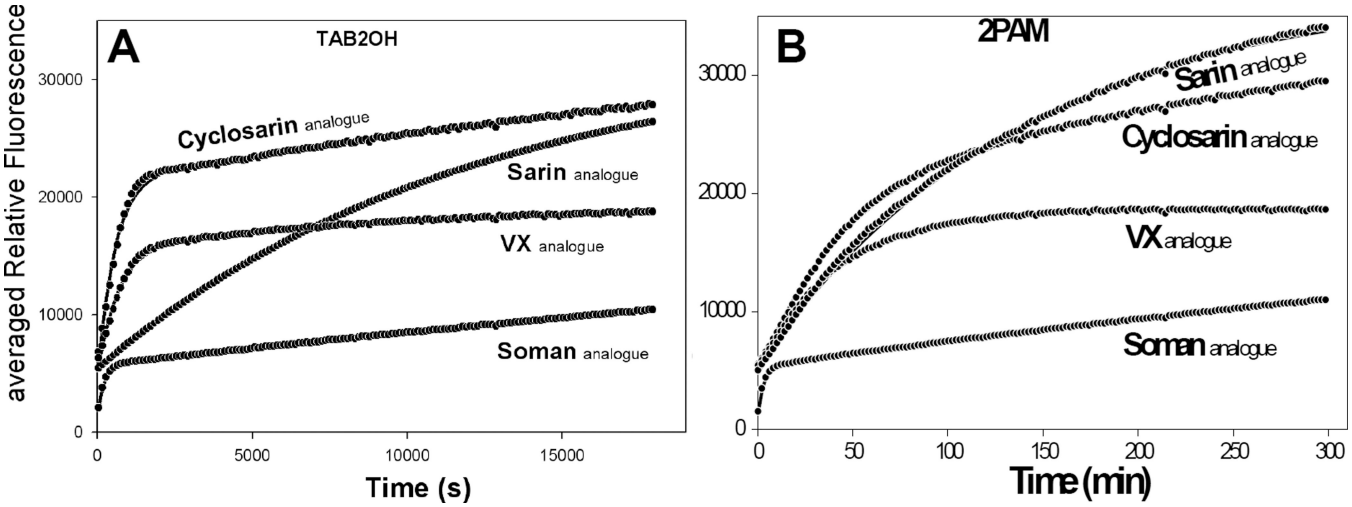

Figure 5.

Time course of nerve agent OP analogue (5 μM) catalytic hydrolysis by 0.1 mM oximes and 500 nM hBChE A) **TAB2OH** and B) 2PAM. Continuous measurements of the increase in fluorescence intensity of fluorescent leaving groups at 37°C in 0.1M Phosphate buffer, pH 7.4. The fluorescent OP leaving group for cyclosarin, sarin and soman analogues was 3-cyano-4-methyl-7-hydroxy coumarin whereas for VX analogue it was 7-hydroxy-9*H*-1,3-dichloro-9,9-dimethylacridine-2-one. Hydrolysis in the absence of oxime or absence of the hBChE was significantly slower and equivalent to or slower than the slow phase of soman or VX analogue hydrolysis.

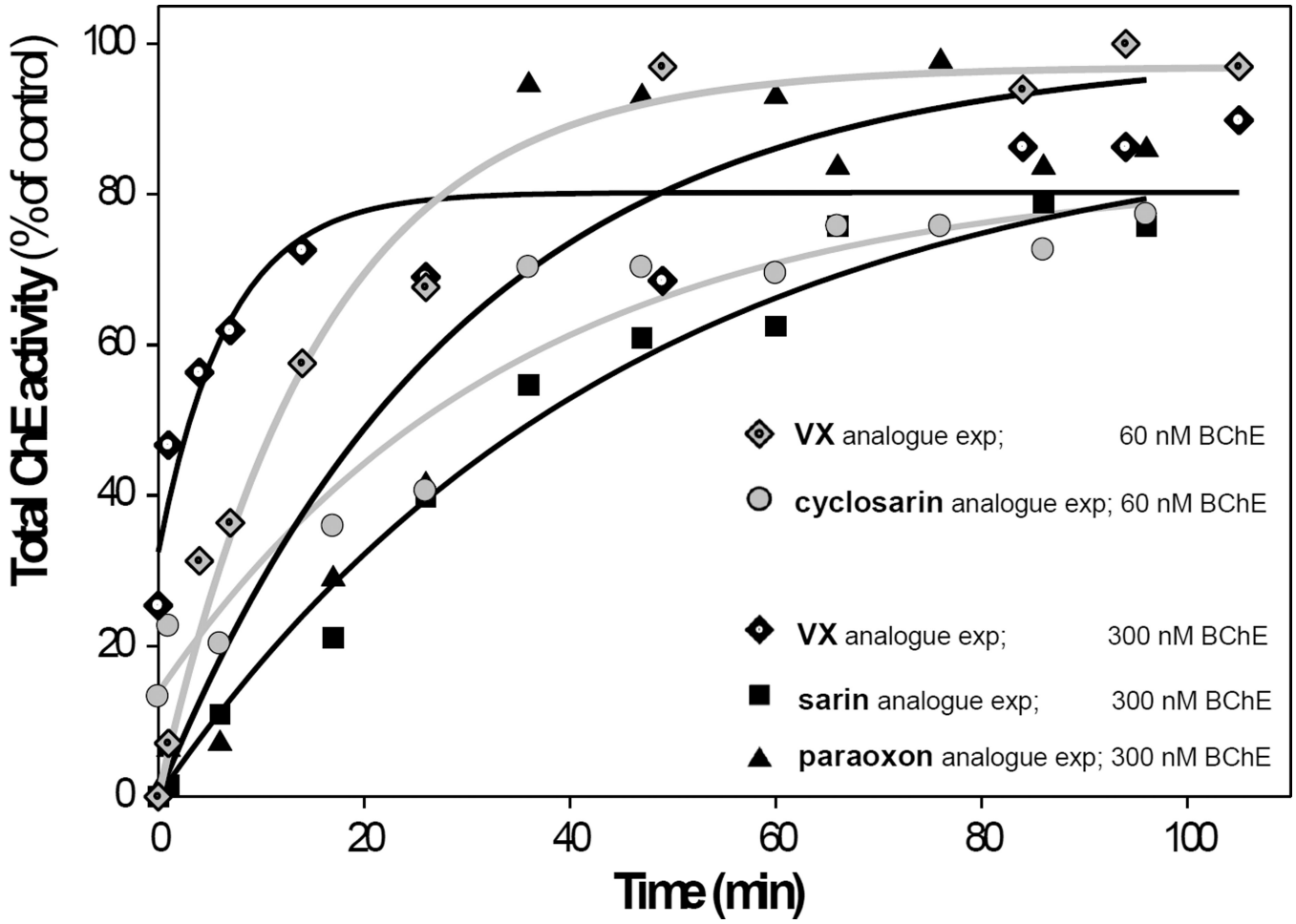

Figure 6.

Recovery of total ChE activity in whole human blood supplemented with 300 nM or 60 nM hBChE and then exposed to nerve agent OP analogues (0.5μM), upon addition of 100 μM oxime **TAB2OH** measured at 37 °C in duplicate. Grey symbols and lines refer to 60 nM hBChE and black symbols and lines to 300 nM hBChE experiments. VX analogue exposure (diamonds), cyclosarin analogue exposure (circles), sarin analogue exposure (squares) and paraoxon exposure (triangles) is shown.

Table 1

Kinetic constants for reactivation of paraoxon-, sarin-, cyclosarin-,VX- and tabun-hBChE and hAChE conjugates by non-pyridinium oxime TAB2OH and reference oxime 2PAM; inhibition constants, K_i and αK_i, (mM),of native AChE and BChE (without OP) by two oximes. Maximal reactivation rate constant (k_2, min^{-1}), apparent dissociation constant of [oxime * OP-hAChE conjugate] reversible complex (K_{ox}, mM) and overall second order reactivation rate constant (k_r, $M^{-1}min^{-1}$) were determined from reactivation curves as presented in Figure 3 and Figure S1. All constants were determined from triplicate experiments in 0.1M phosphate pH 7.4, 37°C. Standard errors of determined kinetic constants were typically less than 30% of the mean.

Oxime	enzyme	Paraoxon			Sarin			Cyclosarin			VX			Tabun			without OP	
		k_2	K_{ox}	k_r	k_2	K_{ox}	k_r	k_2	K_{ox}	k_r	k_2	K_{ox}	k_r	k_2	K_{ox}	k_r	K_i	αK_i
TAB2OH	BChE	0.34	0.71	480	0.19	0.79	250	3.9	1.0	3700	2.0	1.5	1300	0.00027	1.3	0.21	0.32	0.74
2PAM	BChE	0.23	2.4	96	2.4	1.8	1300	2.6	5.4	480	1.2	2.5	480	0.0011	1.2	0.91	0.23	18
TAB2OH	AChE	0.47	12	41	0.92	27	34	0.44	36	12	2.4	23	100	0.0032	8.2	0.39	0.20	4.0
2PAM	AChE	0.27	1.8	150	1.1	0.34	3300	0.73	6.6	110	0.74	0.32	2300	0.0058	1.6	3.8	0.34	1.9

Table 2

Summary of pKa values[a] for ionizable groups in structures of several oximes determined from NMR, spectroscopy, and kinetic parameters.

oxime		method	pK_{a1}	pK_{a2}
			hydroxyl	*oximate*
TAB2OH	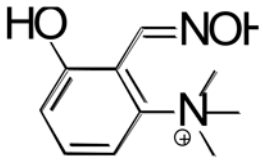	UV 240nm	7.44 ± 0.05	10.6 ± 0.1
		UV 275nm	7.58 ± 0.07	-
		UV 310nm	7.52 ± 0.05	10.1 ± 0.3
		NMR (s)	7.69 ± 0.08	-
		NMR (t)	7.63 ± 0.09	-
		NMR (d1)	7.74 ± 0.08	-
		NMR (d2)	7.70 ± 0.08	-
		NMR (s2)	7.70 ± 0.08	
		oximolysis*	7.21 ± 0.14 (k_{max} = 6 ± 1)	≥ 9.3 (k_{max} ≥ 21)
TAB2	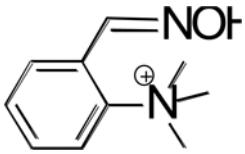	UV 285nm	-	9.47 ± 0.05
		oximolysis*		≥ 10.2 (k_{max} ≥ 250)
TAB4OH	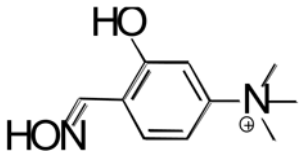	UV 275nm	7.47 ± 0.12	11.03 ± 0.04
		UV 340nm	7.45 ± 0.03	10.93 ± 0.09
		oximolysis*	7.54 ± 0.01 (k_{max} = 15 ± 1)	≥ 10.7 (k_{max} ≥ 65)
TAB4	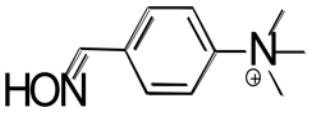	UV 245nm	-	10.13 ± 0.01
		UV 285nm	-	10.09 ± 0.06
		oximolysis*	-	≥ 10.7 (k_{max} ≥440)
Edrophonium	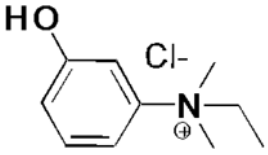	UV 240nm	8.22 ± 0.03	-
		UV 270nm	8.20 ± 0.06	-
		UV 295nm	8.20 ± 0.03	-
		oximolysis	*n.d.* (k_{max} ~ 0)	
2PAM	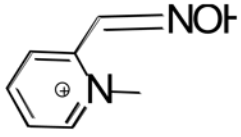	NMR	-	8.11 ± 0.03
		OP oximol	-	8.1 ± 0.2
		oximolysis	-	8.0 ± 0.1 (k_{max} = 60)

[a] pK_a values determined in D_2O (by NMR), are typically higher than those determined in H_2O by ~0.5 c.f.[16] and were accordingly corrected. All pK_a values were determined at room temperature.

[*] pK_{a2} values determined for oximolysis (using nonlinear regression of eq.1 or eq.2) and associated k_{max} values, were presented as "larger or equal" for pK_{a2} values higher than 9 since rates of oximolysis were measured up to pH 10, only.

Table 3

Treatment of OP exposed mice with oxime TAB2OH. The oxime was administered either alone (**Therapy**: *i.m.* 25 mg/kg with atropine 1 min after an OP) or as combination with hBChE (**Pretreatment + Therapy**: *i.v.* [hBChE (1 mg/kg) + TAB2OH (25 mg/kg)] 15 min before OP followed by TAB2OH (25 mg/kg with atropine) administered *i.m.* 1 min after an OP). Protective Index is the ratio of LD_{50} for OP exposed animals with pretreatment/therapy and animals exposed to OP only. In parentheses 95% confident limits of protective index and MDP (the highest multiple of the OP LD_{50}, which was fully counteracted by the antidotal treatment) are also given.

Treatment	VX[a]		Paraoxon[b]		Sarin[c]		Tabun[d]	
	Protective Index (95% conf. limits)	**MDP**	**Protective Index (95% conf. limits)**	**MDP**	**Protective Index (95% conf. limits)**	**MDP**	**Protective Index (95% conf. limits)**	**MDP**
Therapy	5.0 (2.2–11.7)	3.2	10 (7.5–13.3)	6.3	2.9 (2.3–3.7)	2.0	1.6 (1.2–2.1)	1.3
Pretreatment + Therapy	5.0 (3.3–7.7)	3.2	16 (13.5–18.7)	13	4.0 (2.5–6.4)	2.0	1.3 (1.0–1.6)	1.3

[a] s.c. LD_{50} of VX was 28 μg/kg.

[b] s.c. LD_{50} of Paraoxon was 740 μg/kg.

[c] s.c. LD_{50} of Sarin was 240 μg/kg.

[b] s.c. LD_{50} of Tabun was 570 μg/kg.

Table 4

Antidotal efficacy of oxime TAB2OH and human BChE in OP exposed mice. Protective index is the ratio of LD_{50} for OP exposed animals with pretreatment/therapy and animals exposed to OP only. In parentheses 95% confidence limits of Protective Index and MDP (the highest multiple of the OP LD_{50}, which was fully counteracted by the antidotal treatment) are also given.

Pretreatment (i.v.)		Therapy (i.m.)	VX[a]		Paraoxon[b]	
15 min	**30 min**	**1 min after OP**	**Protective Index (95% conf. limits)**	**MDP**	**Protective Index (95% conf. limits)**	**MDP**
		25 mg/kg TAB2OH	1.3 (0.7–2.1)	*1.3*		
		10 mg/kg TAB2OH with atropine	2.7 (2.5–3.0)	*2.5*		
		25 mg/kg TAB2OH with atropine	5.0 (2.2–11.7)	3.2	10.0 (7.5–13.3)	6.3
	0.5 mg/kg hBChE		1.0 (0.9–1.1)	*0.79*		
	1 mg/kg hBChE		1.1 (0.8–1.4)	*nd*	<1.0 (nd)	*nd*
	0.5 mg/kg hBChE	10 mg/kg TAB2OH with atropine	3.4 (2.7–4.4)	*3.4*		
	1 mg/kg hBChE in atropine		2.5 (1.3–4.8)	*1.3*		
	1 mg/kg hBChE	25 mg/kg TAB2OH with atropine	5.0 (3.3–7.7)	3.2	14.1 (12.0–16.7)	10
1 mg/kg hBChE with 25 mg/kgTAB2OH			<1 (nd)	*nd*	<1 (nd)	*nd*
	1 mg/kg hBChE with 25 mg/kg TAB2OH				<1 (nd)	*nd*
1 mg/kg hBChE with 25 mg/kg TAB2OH		25 mg/kg TAB2OH with atropine	5.0 (3.3–7.7)	3.2	16 (13.5–18.7)	13
		1 mg/kg hBChE + 25 mg/kg TAB2OH with atropine			13 (8.2–19.1)	7.9

[a] s.c. LD_{50} of VX was 28 μg/kg.

[b] s.c. LD_{50} of Paraoxon was 740 μg/kg.